Proc. Natl. Acad. Sci. USA
Vol. 83, pp. 3267–3271, May 1986
Biophysics

Distribution of ions around DNA, probed by energy transfer

(fluorescence/rapid-diffusion limit/electrostatics/Poisson–Boltzmann equation/discrete charge algorithm)

THEODORE G. WENSEL*†, CLAUDE F. MEARES*‡, VOJKO VLACHY*, AND JAMES B. MATTHEW§

*Chemistry Department, University of California, Davis, CA 95616; and §Central Research and Development, E.I. DuPont de Nemours, Wilmington, DE 19898

Communicated by John D. Baldeschwieler, December 20, 1985

ABSTRACT **Measurements of the effect of DNA on rates of bimolecular energy transfer between ions provide a direct indication of how cations cluster in regions near DNA and how anions are repelled from the same regions. Energy transfer from luminescent lanthanide ions (in the "rapid-diffusion" limit) probes collision frequencies that are dependent on the equilibrium spatial distributions of ions. The addition of 1 mM DNA (phosphate) to a 2 mM salt solution increases the overall collision frequency between monovalent cations by a factor of 6 ± 1.5; it increases the divalent–monovalent cation collision frequency by a factor of 29 ± 3; and it decreases the divalent cation–monovalent anion collision frequency by a factor of 0.24 ± 0.03. Comparisons are made with the changes in collision frequencies predicted by several different theoretical descriptions of ion distributions. The closest agreement with experimental results for monovalent ions at 1 mM DNA is obtained with a static accessibility-modified discrete charge calculation, based on a detailed molecular model of B-DNA. At high DNA concentration (10 mM), the best results are obtained by numerical solutions of the Poisson–Boltzmann equation for a "soft-rod" model of DNA. Poisson–Boltzmann calculations for a "hard-rod" model greatly overestimate the effects of DNA on collision frequencies, as does a calculation based on counterion-condensation theory.**

The binding of proteins and other ligands to DNA is central to the regulation of many biochemical processes in cells (1). The rate and extent of binding depend exquisitely on the concentrations of ions in the medium (2–5); clearly the interactions between DNA and proteins are strongly influenced by electrostatic effects. In order to analyze specific interactions at the molecular level, an accurate description of the electrostatic forces near DNA is essential.

Theoretical calculations of the electrostatic potential and the distribution of ions around DNA have been carried out by many authors (e.g., refs. 6–14). On the other hand, experimental techniques for studying these properties usually have been limited to observing either the effect of DNA on bulk thermodynamic properties of the solution (6, 15–17) or the dependence of ligand binding on electrolyte concentration (18, 19). NMR spectroscopy of $^{23}Na^+$ can report directly on ions near DNA, but interpretation is complicated because of the mechanisms of nuclear relaxation involved (20–24).

In principle, the effect of a polyelectrolyte on ion–ion collision frequencies can be used to test theoretical descriptions of the distribution of ions around the polyion (25). However, despite numerous reports concerning the effects of polyelectrolytes on bimolecular chemical reaction rates (refs. 26 and 27 and references therein), quantitative comparisons with theory are lacking.

The experimental measurement and analysis of interactions between ions in solution is straightforward using energy transfer in the rapid-diffusion limit (28–30). With terbium chelates as donors, and simple transition-metal complexes as acceptors, the energy transfer rate depends on the donor–acceptor collision frequency (30). Ion–ion energy-transfer rates in the presence of a polyelectrolyte like DNA depend directly on the spatial distribution of the ions around each DNA molecule. For example, adding DNA should enhance the rate of energy transfer from one cation to another, due to clustering of cations near DNA.

RATIONALE

Relation Between Ion Distributions and Energy-Transfer Measurements. Energy transfer in the rapid-diffusion limit can be used to probe equilibrium properties of solutions, such as ion distributions, because the lifetime of the observed luminescence (≈1 msec) is very long compared to the time required for an ion to diffuse through a representative sample of the solution. As a consequence, all energy donors experience the same average environment (28, 29). We have found experimentally that the rapid-diffusion limit pertains to ions in DNA solutions (see below), as might have been expected from theoretical considerations of the rapid exchange of ions between domains near and far from polyelectrolytes (24).

In the rapid-diffusion limit all donors are effectively equivalent, so that after a pulse of exciting light a single exponential decay of luminescence is observed:

$$-\frac{dC_i}{dt} = C_i\frac{1}{\tau} = C_i\left[\frac{1}{\tau_0} + k_0C_j\right], \qquad [1]$$

where C_i is the concentration of excited donor, τ_0 is the unquenched lifetime measured in the absence of acceptor, C_j is the concentration of energy acceptor, and k_0 (M^{-1} sec^{-1}) is the second-order rate constant for energy transfer.

It can be shown easily (31) that if k is the observed rate constant for i–j energy transfer in the presence of a polyelectrolyte and k_0 is the rate constant in its absence, these rate constants for energy transfer between small ions are related as follows:

$$k/k_0 = \frac{\int C_i(r)C_j(r)dV/\int dV}{[\int C_i(r)dV/\int dV][\int C_j(r)dV/\int dV]}, \qquad [2]$$

where the domain of integration extends over all space accessible to small ions. For reactions much slower than the diffusion-controlled limit ($k_0 << 10^{10}$ M^{-1} sec^{-1}), an equilibrium expression may be used for $C_i(r)$. In the following analyses, we make the approximation that the distributions of different ions (e.g., donor and acceptor cations) are indepen-

The publication costs of this article were defrayed in part by page charge payment. This article must therefore be hereby marked "*advertisement*" in accordance with 18 U.S.C. §1734 solely to indicate this fact.

Abbreviations: Bu_4N^+, tetrabutylammonium; PB, Poisson–Boltzmann; SA-TK, static accessibility-modified discrete charge algorithm.

†Present address: Department of Cell Biology, Stanford University School of Medicine, Stanford, CA 94305.
‡To whom reprint requests should be addressed.

dent (i.e., uncorrelated) and determined strictly by ion charge and size.

In a polyelectrolyte solution, the equilibrium local concentration of ions in the polyion reference frame can be described by a Boltzmann factor that accounts for the effects of all interparticle interactions:

$$C_i(r) = C_i^0 \, e^{-w_i(r)/k_B T}, \qquad [3]$$

where $C_i(r)$ is the local concentration of ions of type i at position r with respect to the polyion, $w_i(r)$ is the potential of mean force acting on such ions, k_B is Boltzmann's constant, and T is the absolute temperature. C_i^0 is the concentration when $w_i(r) = 0$.

Since Eqs. 2 and 3 apply to second-order rate constants for collisional energy transfer in the rapid-diffusion limit, experimental measurements of k/k_0 can be compared with theoretical predictions of $C_i(r)$. It should be noted that collisional processes—not the through-space dipolar mechanism—are dominant for the experiments described here (30–36).

Counterion-Condensation Calculation. This approach, developed by Manning (12, 13), has proven widely useful in relating experimental results to the electrostatic properties of DNA (refs. 6, 12, 13 and references therein). Its central hypothesis is that a condensed layer of counterions is clustered around each DNA molecule, so that the phosphate charges are largely neutralized. For DNA at 25°C, the average net charge per phosphate is predicted to be 0.24 of its full value.

To obtain a lower limit on the effect of DNA on energy transfer predicted by this theory, we assumed a simplified distribution of ions (described in the legend to Fig. 1). It can be shown (31) that for this model, Eq. 2 may be replaced by

$$k/k_0 = \frac{0.76\,\bar{C}_{DNA}(1.2\text{ M})}{(\bar{C}_{+1})^2} + \left[1 - \frac{0.76\,\bar{C}_{DNA}}{\bar{C}_{+1}}\right]^2 \qquad [4]$$

for energy transfer between monovalent cations, where $\bar{C}_{+1}$ is the total molar concentration of monovalent cations, and $\bar{C}_{DNA}$ is the total molar concentration of DNA phosphate residues. The results are compared with the other calculations in Table 2 and the figure legends.

Poisson–Boltzmann (PB) Hard- and Soft-Rod Calculations. The distribution profile $C_i(r)$ in Eq. 3 can be calculated using the cell model of polyelectrolyte solutions, together with the PB equation (37). The statistical-mechanical approximations involved in the PB equation and the cell model have been examined recently (9, 38–42). The DNA solution is modeled as an ensemble of cylindrical cells of radius R (Å) and length L (Å), with the polyions placed along the cell axes. The negative DNA molecules are assumed to be uniformly charged cylinders, each surrounded by a positively charged "atmosphere" of pointlike ions. The cell radius is determined by the molar concentration, $\bar{C}_{DNA}$, of monomer units (or phosphate) in the solution:

$$\bar{C}_{DNA} = \frac{10^{27}\nu}{\pi(R^2 - a^2)LN_A}. \qquad [5]$$

Here ν/L is the number of nucleotides per unit length of DNA [(1.7 Å)$^{-1}$], N_A is Avogadro's number, and a is the polyion–small ion contact distance (a = 14 Å if the small ion has a 4-Å radius). For $\bar{C}_{DNA}$ = 1 mM, R = 558 Å; for $\bar{C}_{DNA}$ = 10 mM, R = 176 Å.

The PB equation for this system is

$$\frac{1}{r}\frac{d}{dr}\left[r\,\frac{d\psi(r)}{dr}\right] = -\frac{e}{\varepsilon}\sum_i Z_i C_i(r), \qquad [6]$$

where r is the distance from the polyion axis, $\psi(r)$ is the mean electrostatic potential, e is the magnitude of the electron charge, the dielectric constant ε is 78.5, and $Z_i e$ is the charge on ion i. The boundary conditions

$$\left[\frac{d\psi(r)}{dr}\right]_R = 0 \qquad [7a]$$

and

$$\left[\frac{d\psi(r)}{dr}\right]_a = \frac{\nu e}{2\pi\varepsilon a L} \qquad [7b]$$

follow from Gauss' law.

In order to solve Eq. 6, it is necessary to relate $C_i(r)$ to $\psi(r)$. The usual (mean-field) approximation is to set $w_i(r) = Z_i e\psi(r) + u_i(r)$ in Eq. 3, where $u_i(r)$ accounts for the exclusion of small ions from the interior of the polyion. For a "hard" polyion, $u_i(r) = \infty$ if $r < a$, and $u_i(r) = 0$ if $r \geq a$. Alternatively, for a "soft" polyion, $u_i(r) \doteq 0.8\,k_B T\,(a/r)^9$ (40). Fig. 1 shows how $w_i(r)$ depends on r for these models.

SA-TK Molecular Model Calculation. In contrast to the charged-cylinder approximation, the static accessibility-modified discrete charge algorithm (SA-TK) (43, 44) uses the molecular structure of B-DNA (11, 45, 46). The semiempirical SA-TK model employs a calculated solvent accessibility (47) to approximate the effect of partitioning the DNA charges across a macroscopic dielectric boundary (48).

The electrostatic potential $\psi(r_m)$, resulting from the phosphate charges $Z_l e$ at positions r_l on the DNA molecule, is calculated at any point r_m outside the van der Waals surface of the DNA according to

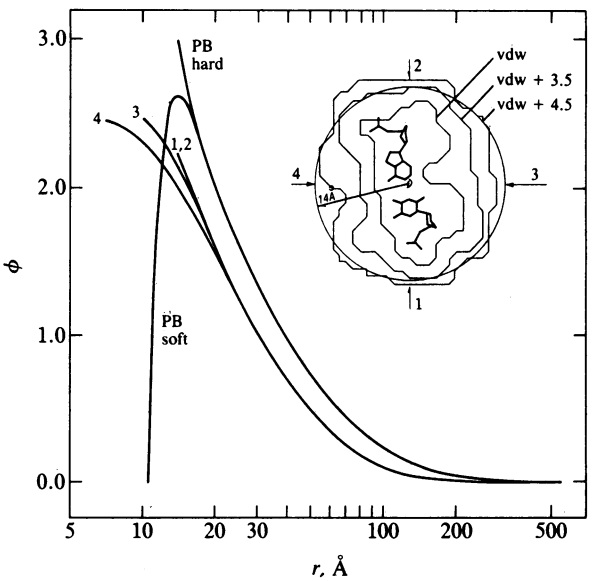

FIG. 1. The potential $\phi = -w_i(r)/2.303\,k_B T$ as a function of distance r from the DNA axis, for 1 mM DNA (phosphate) and 2 mM added salt. The predicted PB distributions for a uniform charged cylinder (14 Å radius) with impenetrable (PB hard) or "soft" solvent boundary conditions are shown, as are the SA-TK molecular model computations (curves 1–4) for the directions given in the *Inset*. (*Inset*) A single base pair with three irregular surfaces corresponding to the van der Waals surface (inner) and the exclusion surfaces for probe ions of radius 3.5 Å and 4.5 Å. Curves 1–4 terminate at the 3.5 Å surface. Not shown is the distribution assumed in the counterion-condensation calculation; this would be a step function with ϕ = 2.8 for 14 Å $\leq r \leq$ 21 Å and ϕ = 0.05 for $r >$ 21 Å.

$$\psi(r_m) = \sum_{l=1}^{N} \frac{Z_l e}{|r_m - r_l| \varepsilon_{lm}^{\text{eff}}} \quad [8]$$

Here $\varepsilon_{lm}^{\text{eff}}$ represents the effective dielectric value between points l and m. As discussed in ref. 11, for any position r_m outside the dielectric boundary of DNA, $\varepsilon_{lm}^{\text{eff}}$ can be taken as $50(1 - SA_l)^{-1/2} \exp(\kappa|r_m - r_l|)$, where $SA_l = 0.75$ is the fractional static solvent accessibility of DNA charge site l, computed from the molecular structure of B-DNA. [Note that the factor $(1 - SA_l)^{-1/2}$ is missing from equation 4 of ref. 11.]

The Debye–Hückel parameter κ used in $\varepsilon_{lm}^{\text{eff}}$ depends on ionic strength (μ); for aqueous solutions at 25°C, $\kappa = 0.33 (\mu)^{1/2}$ Å^{-1}. The SA-TK calculation was developed for infinitely dilute solutions of macromolecules, where the ionic strength may be calculated directly from the concentration of added salt. To extend the calculation to the finite concentrations of DNA used in these experiments, we briefly investigated the effect of varying the value of μ used to calculate κ (Table 2). The dependence of energy transfer on added salt (Fig. 2) and DNA (Fig. 3) is described in a consistent way by using $\mu = 1$ mM + C^0, where C^0 is the concentration of added salt.

The calculation of electrostatic potential as a function of distance from the DNA charges is carried out numerically, on a 1-Å orthogonal grid. Grid points near the DNA's van der Waals surface that are sterically inaccessible to the charged donors and acceptors are excluded from the calculation. Eqs. **2** and **3** are then used to compute k/k_0, after substituting $w_i(r_m) = Z_i e \psi(r_m)$. The computation is carried out over five contiguous 1-Å-thick cross-sections through the middle of a 40-base-pair DNA segment, extending to the limit of radial integration (R in Eq. **5**).

These calculations predict the highest concentration of mobile cations in the minor groove of DNA. These ions are treated as a localized or "bound" equilibrium population, which is taken into account in the calculation (11). For the experimental conditions reported here, this population is always <0.10 cation per phosphate charge. The exchange rate between cation populations is not addressed in the computations; however, if exchange occurs on a submillisecond time scale, the criteria for the rapid diffusion limit are met.

MATERIALS AND METHODS

Calf thymus DNA [tetrabutylammonium (Bu_4N^+) salt] was prepared as described (31, 36). The ratio A_{260}/A_{280} was 1.9, and hyperchromicity at 260 nm upon melting was 29%. The buffer contained 1.0 mM *N*-2-hydroxyethylpiperazine-*N'*-2-ethanesulfonic acid (the Bu_4N^+ salt was used because the radius of this cation is about 4 Å), pH 7.0. The values given for added salt (usually 2.0 mM) include buffer, donors, acceptors, and added $Bu_4N^+Br^-$ but did not include DNA and its complement of cations.

The energy donor used in each energy-transfer experiment was one of the following terbium chelates (0.5 mM), prepared as described (31, 35): −1 donor, ethylenediaminetetraacetatoterbiate(III); neutral donor, hydroxyethylethylenediaminetriacetatoterbium(III); +1 donor, bis(hydroxyethyl)-ethylenediaminediacetatoterbium(III). These complexes have similar structures and sizes (roughly spherical with a radius of ≈4 Å) and have been found to behave in energy-transfer experiments as if they differed only in net charge (35).

The energy acceptor used in each case was one of a series of transition-metal complexes with roughly spherical shape and 4-Å radius (31): −1 acceptor, ethylenediaminetetraacetatocobaltate(III) (49); neutral acceptor, bis(hydroxyethyl)-ethylenediaminediacetatocopper(II) (35); +1 acceptor, *sym*-*cis*-ethylenediaminediacetato(ethylenediamine)cobalt(III) (50); +2 acceptor, 2-mercaptoethylaminebis(ethylenediamine)cobalt(III) (51). The concentrations of acceptors ranged from 25 μM (+2 acceptor/+1 donor) to 0.5 mM (neutral acceptor/+1 donor). In confirmation of the 4-Å radii of the donors and acceptors, distances of closest approach were determined to be 7–8 Å by the methods described previously (30, 31, 34).

Rates of energy transfer were determined from measurements of Tb(III) luminescence lifetimes in the presence and absence of acceptors, using the instrument described previously (31, 35). Samples were thermostatted at 25°C.

RESULTS

The effects of DNA on energy transfer between donors and acceptors with various charges are shown in Table 1. The results all qualitatively conform to the behavior expected for small ions in the presence of a negative polyelectrolyte. For example, cation-clustering around the DNA results in enhanced energy-transfer rates between monovalent cations ($k/k_0 = 6$) and even greater enhancement for a divalent cation acceptor and a monovalent cation donor ($k/k_0 = 29$). In contrast, DNA reduces energy transfer between the divalent cation energy acceptor and the anionic energy donor ($k/k_0 = 0.24$) by repelling the negative donor from the region near its surface (where the positive acceptor is most concentrated). DNA has no significant effect on the experiments involving an electrically neutral donor or acceptor, confirming the electrostatic nature of the process. Evidently, nonelectrostatic effects due to structural differences between donors and acceptors are not large enough to affect the results significantly; for example, k/k_0 for the −1/+1 pair is equal, within experimental error, to k/k_0 for the +1/−1 pair.

By demonstrating the effects of ion charge, salt concentration, and DNA concentration, the experimental data provide an excellent test of theoretical predictions. It is clear from Table 2 and Figs. 2 and 3 that none of the calculations presented here fits all the data. The SA-TK treatment agrees reasonably well with experimental measurements of salt dependence at 1 mM DNA (Fig. 2*A*) and DNA dependence at 2 mM salt (Fig. 3). However, Fig. 2*B* shows that this approach is not adequate for describing the salt dependence at 10 mM DNA.

At 10 mM DNA, the best agreement with experiment is obtained with the PB calculations for the soft-rod model. But the soft-rod calculation considerably overestimates the measured data for conditions of low DNA (1 mM) and low salt, as well as for the DNA dependence (Fig. 3). In every case, the PB soft-rod model gives better agreement with experiment than does the hard-rod model, and even the PB hard-rod model gives better agreement than the counterion condensation calculation (see legends to Figs. 2 and 3).

Substantial discrepancies occur between experimental results and all the theories for the +2 acceptor/+1 donor pair (Table 2); neither the SA-TK nor the PB calculations were modified to take the presence of 25 μM divalent cations into account.

Table 1. Ratios of energy-transfer rate constants (k/k_0) measured for different donor–acceptor charge combinations, in 2 mM salt ± 1 mM DNA (phosphate)

	k/k_0		
Acceptor	+1 Donor	0 Donor	−1 Donor
+2	29 ± 3	0.95 ± 0.1	0.24 ± 0.03
+1	6.0 ± 1.5	1.0 ± 0.1	1.0 ± 0.04
0	1.0 ± 0.1	1.0 ± 0.05	1.0 ± 0.05
−1	0.9 ± 0.1	1.0 ± 0.1	1.0 ± 0.1

Error limits represent one standard deviation.

Table 2. Comparison of theoretical predictions and experimental results for effects of DNA on ion–ion energy transfer, for 2 mM salt ± 1 mM DNA

Ion charges (acceptor/donor)	k/k_0				
	PB		SA-TK		Experimental
	Hard	Soft	4.5 Å*	3.5 Å*	
+1/+1†	52.4‡	33.7	9.9§	15.6§	6 ± 1.5
			5.4¶	8.2¶	
			3.6‖	5.3‖	
−1/+1	0.74	0.74	0.91¶	0.89¶	0.9 ± 0.1
+1/−1					1.0 ± 0.04
+2/+1**	403	209	78.7¶	113.7¶	29 ± 3
+2/−1**	0.014	0.022	0.17¶	0.11¶	0.24 ± 0.03

*Probe radius.
†Counterion-condensation prediction: $k/k_0 = 102$.
‡For ions of radius 4 Å. Changes to 25 if donor and acceptor ions differ in radius by 1.5 Å.
§Ionic strength $\mu = 2$ mM used in κ in ε_{lm}^{eff} (Eq. 8).
¶$\mu = 3$ mM used in κ in ε_{lm}^{eff} (Eq. 8).
‖$\mu = 4$ mM used in κ in ε_{lm}^{eff} (Eq. 8).
**These theoretical calculations do not take into account changes in the potential caused by the presence of divalent cations.

DISCUSSION

It is important to consider whether the experimental results accurately reflect ion distributions as discussed above. If donor cations clustered near the DNA are not in rapid equilibrium (on a millisecond time scale) with the ions in the bulk solution, then more complex treatment of the data would be required. Several experimental tests of donor binding to DNA have been described (31, 36). Among the results is the fact that, over a wide range of donor and acceptor concentrations, each luminescence decay is accurately fit by a single exponential (correlation coefficient > 0.999), indicating that all donors are in equivalent average environments. These results imply that binding to DNA is not significant for the present experiments; however, they do not rule out the possibility of small numbers of transiently bound donor or acceptor cations (e.g., as postulated in the SA-TK calculations).

In the PB hard-rod calculations, the assumption that DNA is an impenetrable cylinder leads to the prediction of a very high concentration of counterions in contact with the polyion (Fig. 1; ref. 40). At low salt concentrations, the major contribution to Eq. 2 stems from a domain less than 10 Å from the polyion surface; thus accurate modeling of this region is critical for predicting the energy-transfer results. It is significant that both hard-rod and soft-rod PB calculations give better predictions at high DNA concentrations. Under these conditions (10 mM DNA) the average concentration of cations in the solution is much higher than for 1 mM DNA with the same amount of added salt. Consequently, the cation distribution $C_i(r)$ is less dramatically nonuniform, and the contribution of ions close to the DNA surface is statistically less important.

Modifications to the PB equation can be made to account for some of the effects which it neglects, such as ion–ion correlations and dielectric saturation; these lead to predictions of higher values for k/k_0 for +1/+1 energy transfer than predicted by the unmodified PB equation. More rigorous calculations (e.g., the hypernetted-chain equation, ref. 42) for a similar model predict a slightly higher value of k/k_0; Monte Carlo calculations based on the same model agree well with PB calculations (V.V., unpublished results). Further, in our analysis of +1/+1 energy transfer, we have assumed exactly the same distribution function for acceptors and donors. A mismatch of distributions, due to unequal ionic radii or noncoulombic interactions, could change the results significantly (PB, Table 2).

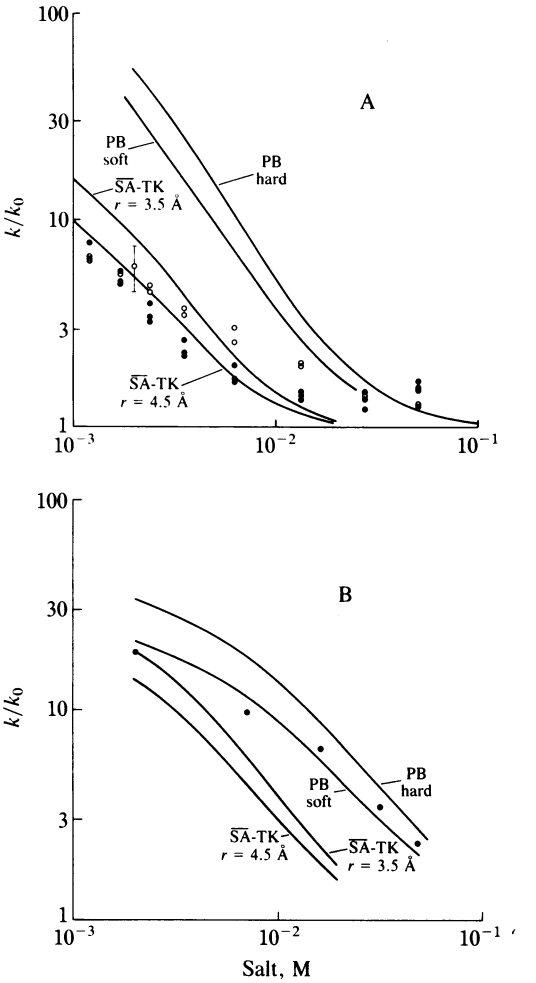

FIG. 2. Salt dependence of DNA-enhanced energy transfer between monovalent cations. The ratio of the rate constant for energy transfer in the presence of 1 mM (*A*) or 10 mM (*B*) DNA (phosphate) to the rate constant in the absence of DNA (k/k_0) is plotted as a function of added salt. Either the +1 donor salt (● in *A*) or $(Bu)_4N^+Br^-$ (○ in *A*, ● in *B*) was used to increase the salt concentration from 2 to 50 mM. In *A*, three independent titrations with the +1 donor salt are shown, and two with $(Bu)_4N^+Br^-$. The point for 2.0 mM added salt was measured six times; the mean value is indicated along with an error bar for the standard deviation. Theoretical PB and SA-TK curves are shown. The counterion-condensation predictions of k/k_0 are a factor of 2.0 higher than the PB-hard value at 2 mM salt and a factor of 1.2 higher than the PB-hard value at 50 mM salt.

The semiempirical SA-TK theory has been successful in describing a number of electrostatic effects in macromolecules (43, 52–55). The SA-TK model was originally developed in the context of an infinitely dilute macromolecule and does not explicitly include the effect of DNA concentration. In Eq. 8, the effect of electrolyte concentration on $\psi(r)$ is included as a simple "effective" ionic strength, μ, in the Debye–Hückel parameter κ in ε_{lm}^{eff}. The SA-TK computation is most appropriately applied to conditions where the combination of DNA concentration and Debye screening from added salt approximates infinite dilution (i.e., the radius of integration R exceeds the radius at which the electrolyte concentration is perturbed by DNA). Both the PB and the SA-TK calculations illustrated in Fig. 1 indicate that this is the case for 1 mM DNA plus 2 mM added salt, since over a large fraction (0.75) of the cell volume, the cation concentration is nearly unperturbed by the presence of the DNA [C_+

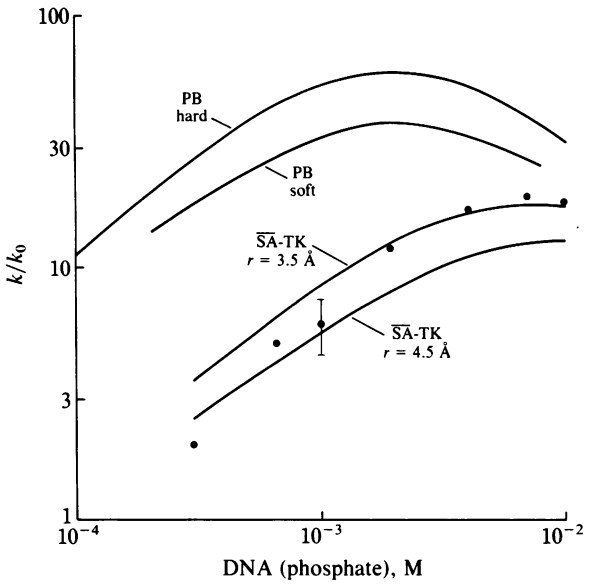

FIG. 3. Rate-constant ratio (k/k_0) for energy transfer between monovalent cations as a function of DNA concentration. Energy-transfer rate enhancement increases from about 2 at 0.3 mM DNA to a maximum k/k_0 value of almost 20 at 7–10 mM DNA. Except for the addition of DNA, the sample compositions were identical. Total added salt concentration was 2.0 mM. The value of k/k_0 predicted by the counterion-condensation calculation is uniformly higher than the PB-hard prediction, by a factor of 1.9.

(280 Å) = 2.16 mM, and C_+ (557 Å) = 2.1 mM]. However, for 2 mM added salt and 10 mM DNA, at the limit of integration (R = 176 Å) the cation concentration is still nearly twice the added salt concentration.

It is interesting to ask which aspects of the SA-TK calculation are responsible for its marked variance with the PB calculation. If the charged sites in the SA-TK calculation are projected onto the axis of a cylinder of radius 14 Å (uniform dielectric ε = 78.5, no ion localization), the predicted k/k_0 becomes 42. This approximates the answer obtained for the PB hard rod, 52.4. Changing from a charged cylinder to the B-DNA structure, still with uniform dielectric and no ion localization, SA-TK predicts a k/k_0 of 66 for 4.5-Å probe ions. Introduction of the macroscopic dielectric boundary and solvent accessibilities reduces the predicted k/k_0 to 10.9. Finally, inclusion of ion localization in the minor groove reduces k/k_0 to 5.4.

We thank Charles Anderson, Charles Woodbury, Donald McQuarrie, C.-H. Chang, and George Pack for advice and helpful discussions. This work was supported by Research Grant GM25909 to C.F.M. and a stipend to T.G.W. from Training Grant GM07377 from the National Institutes of Health and by Research Instrumentation Grant CHE81-14966 from the National Science Foundation.

1. Lewin, B. (1983) *Genes* (Wiley, New York).
2. Riggs, A. D., Suzuki, H. & Bourgeois, S. (1970) *J. Mol. Biol.* **48**, 67–83.
3. Winter, R. B., Berg, O. G. & Von Hippel, P. H. (1981) *Biochemistry* **20**, 6961–6977.
4. DeHaseth, P. L., Lohman, T. M. & Record, M. T., Jr. (1977) *Biochemistry* **16**, 4783–4790.
5. Roe, J. H., Burgess, R. R. & Record, M. T., Jr. (1984) *J. Mol. Biol.* **176**, 495–522.
6. Anderson, C. F. & Record, M. T., Jr. (1982) *Annu. Rev. Phys. Chem.* **33**, 191–222.
7. Gueron, M. & Weisbuch, G. (1980) *Biopolymers* **19**, 353–382.
8. Granot, J. (1983) *Biopolymers* **22**, 1831–1841.
9. LeBret, M. & Zimm, B. H. (1984) *Biopolymers* **23**, 271–285.
10. Klein, B. J. & Pack, G. R. (1983) *Biopolymers* **22**, 2331–2352.
11. Matthew, J. B. & Richards, F. M. (1984) *Biopolymers* **23**, 2743–2759.
12. Manning, G. S. (1978) *Q. Rev. Biophys.* **11**, 179–246.
13. Manning, G. S. (1979) *Acc. Chem. Res.* **12**, 443–449.
14. Pullman, A. & Pullman, B. (1981) *Q. Rev. Biophys.* **14**, 289–380.
15. Gross, L. M. & Strauss, U. P. (1966) in *Chemical Physics of Ionic Solutions*, eds. Conway, B. E. & Barradas, R. G. (Wiley, New York), pp. 361–389.
16. Shack, J., Jenkins, R. J. & Thompsett, J. M. (1952) *J. Biol. Chem.* **198**, 85–92.
17. Anderson, C. F. & Record, M. T., Jr. (1980) *Biophys. Chem.* **11**, 353–360.
18. Record, M. T., Jr., Anderson, C. F. & Lohman, T. M. (1978) *Q. Rev. Biophys.* **11**, 103–178.
19. Record, M. T., Jr., Mazur, S. J., Melancon, P., Roe, J. H., Shaner, S. L. & Unger, L. (1981) *Annu. Rev. Biochem.* **50**, 997–1024.
20. Reuben, J., Shporer, M. & Gabbay, E. J. (1975) *Proc. Natl. Acad. Sci. USA* **72**, 245–247.
21. Anderson, C. F., Record, M. T., Jr., & Hart, P. A. (1978) *Biophys. Chem.* **7**, 301–316.
22. Bleam, M. L., Anderson, C. F. & Record, M. T., Jr. (1980) *Proc. Natl. Acad. Sci. USA* **77**, 3085–3089.
23. Bleam, M. L., Anderson, C. F. & Record, M. T., Jr. (1983) *Biochemistry* **22**, 5418–5425.
24. Halle, B., Wennerström, H. & Picullel, L. (1984) *J. Phys. Chem.* **88**, 2482–2494.
25. Morawetz, H. (1960) *J. Polym. Sci.* **42**, 125–127.
26. Morawetz, H. (1970) *Acc. Chem. Res.* **3**, 354–360.
27. Baumgartner, E. & Fernandez-Prini, R. (1976) in *Polyelectrolytes*, eds. Frisch, K. C., Lemper, D. & Patsis, A. (Technomic, Westport, CT), pp. 1–33.
28. Stryer, L., Thomas, D. D. & Meares, C. F. (1982) *Annu. Rev. Biophys. Bioeng.* **11**, 203–222.
29. Thomas, D. D., Carlsen, W. F. & Stryer, L. (1978) *Proc. Natl. Acad. Sci. USA* **75**, 5746–5750.
30. Meares, C. F., Yeh, S. M. & Stryer, L. (1981) *J. Am. Chem. Soc.* **103**, 1607–1609.
31. Wensel, T. G. (1984) Dissertation (Univ. of California, Davis).
32. Förster, T. (1948) *Ann. Phys. (Leipzig)* **2**, 55–75.
33. Dexter, D. L. (1953) *J. Chem. Phys.* **21**, 836–850.
34. Meares, C. F. & Rice, L. S. (1981) *Biochemistry* **20**, 610–617.
35. Wensel, T. G. & Meares, C. F. (1983) *Biochemistry* **22**, 6247–6254.
36. Wensel, T. G., Chang, C. H. & Meares, C. F. (1985) *Biochemistry* **24**, 3060–3069.
37. Alexandrowicz, Z. & Katchalsky, A. (1963) *J. Polym. Sci.* **A1**, 3231–3260.
38. Fixman, M. (1979) *J. Chem. Phys.* **70**, 4995–5005.
39. Bratko, D. & Vlachy, V. (1982) *Chem. Phys. Lett.* **90**, 434–438.
40. Bacquet, R. & Rossky, P. J. (1984) *J. Phys. Chem.* **88**, 2660–2669.
41. Linse, P. & Jönsson, B. (1983) *J. Chem. Phys.* **78**, 3167–3176.
42. Vlachy, V. & McQuarrie, D. A. (1985) *J. Chem. Phys.* **83**, 1927–1932.
43. Matthew, J. B., Flanagan, M. A., Garcia-Moreno, E. B., March, K. L., Shire, S. J. & Gurd, F. R. N. (1985) *CRC Crit. Rev. Biochem.* **18**, 91–197.
44. Matthew, J. B. (1985) *Annu. Rev. Biophys. Bioeng.* **14**, 387–417.
45. Matthew, J. B. & Ohlendorf, D. H. (1985) *J. Biol. Chem.* **260**, 5860–5862.
46. Arnott, S. (1981) in *Topics in Nucleic Acid Structure*, ed. Neidle, S. (Macmillan, London) pp. 65–82.
47. Lee, B. K. & Richards, F. M. (1971) *J. Mol. Biol.* **55**, 379–400.
48. Matthew, J. B., Hanania, G. I. H. & Gurd, F. R. N. (1978) *Biochem. Biophys. Res. Commun.* **81**, 410–415.
49. Shimi, I. A. W. & Higginson, W. C. E. (1958) *J. Chem. Soc.* 260–263.
50. Halloran, L. J., Gillie, A. L. & Legg, J. I. (1978) *Inorg. Synth.* **18**, 103–111.
51. Nosco, D. L. & Deutsch, E. (1982) *Inorg. Synth.* **21**, 19–23.
52. Weber, P. C. & Tollin, G. (1985) *J. Biol. Chem.* **260**, 5568–5573.
53. Matthew, J. B. & Richards, F. M. (1982) *Biochemistry* **21**, 4989–4999.
54. Matthew, J. B., Weber, P. C., Salemme, F. R. & Richards, F. M. (1983) *Nature (London)* **301**, 169–171.
55. Steitz, T. A., Weber, I. T. & Matthew, J. B. (1982) *Cold Spring Harbor Symp. Quant. Biol.* **47**, 419–426.